Geotechnical Aspects of Underground Construction in Soft Ground – Elshafie, Viggiani & Mair (eds)
© 2023 ISSMGE, London, UK, ISBN 978-1-032-40947-4

Long term additional load on a shield tunnel in soft clay due to clay consolidation with water leakage

Shigeaki Oka & Jin Saito
Tokyo Electric Power Company Holdings, Inc., Tokyo, Japan

Yoshihiro Ito, Wei Li & Shunsuke Kaneko
Tokyo Electric Power Services Co., Ltd., Tokyo, Japan

Alireza Afshani & Hirokazu Akagi
Department of Civil Engineering, Waseda University, Tokyo, Japan

ABSTRACT: In soft clay ground, shield tunnels suffer from additional load which is generated due to the consolidation of ground caused by water leakage into the tunnel. Therefore, it is important to make precise predictions of future additional loads when designing tunnel reinforcements. In this paper, the mechanism governing the additional load increase was clarified via three-dimensional FEM analysis. Moreover, a simple method to predict the convergence value of additional loads is proposed, comparing the calculation results of a two-dimensional analysis with the three-dimensional analysis.

1 INTRODUCTION

Noteworthy damage was found in a tunnel which was constructed in soft clay in Saitama, Japan in 1981. As shown in Figure 1, several longitudinal cracks on a segment were found in this tunnel. The reason for these cracks is thought to be that the vertical earth pressure acting on the tunnel exceeded the design earth pressure due to consolidation of the ground around it. Moreover, it was thought that the consolidation was induced by water leakage into the tunnel. In this paper, this increased earth pressure is called "additional load." Once this additional load exceeds the design capacity of a tunnel, appropriate reinforcement is needed. Therefore, it is important to predict by how much the additional load will increase in order to plan maintenance for tunnels constructed in soft clay.

In this study, we aimed to clarify the following two points. The first is how water leakage into the tunnel will increase as the tunnel ages. The second is how to predict the future change in additional load. By clarifying these points, we concluded that the reinforcement of this tunnel should be appropriately planned.

In terms of the background to this study, a three-dimensional soil-water coupled FEM analysis was carried out to clarify the mechanism of the water leakage increase and the convergence of additional load on top of the target tunnel. Furthermore, we devised how to calculate the convergence value of the additional load with high accuracy using a simple method based on two-dimensional soil-water coupled FEM analysis. The proposed method can be applied not only to the target tunnel, but also other aged tunnels.

2 OUTLINE OF THE TARGET TUNNEL

The target tunnel is a shield tunnel for underground power transmission, which was constructed in 1981. This tunnel contained several underground transmission cables, as shown in Figure 2. As summarized in Table 1, the lining was composed of reinforced concrete segments. The longitudinal profile of the tunnel was as shown in Figure 3, and the tunnel was constructed in soft clay, the N-value of which is 0~3. The target section in this study is between ventilation shafts No. 4 and No. 5, in which noteworthy water leakage and deformation were observed.

3 PREVIOUS RESEARCH

As shown in Figure 4, Arrizumi et al. (2006) carried out a centrifugal experiment with a model tunnel composed of porous stones that simulates this target tunnel. In this experiment, it was assumed that water leakage occurred from the top, side and bottom of the tunnel from the start of the experiment. As

DOI: 10.1201/9781003355595-46

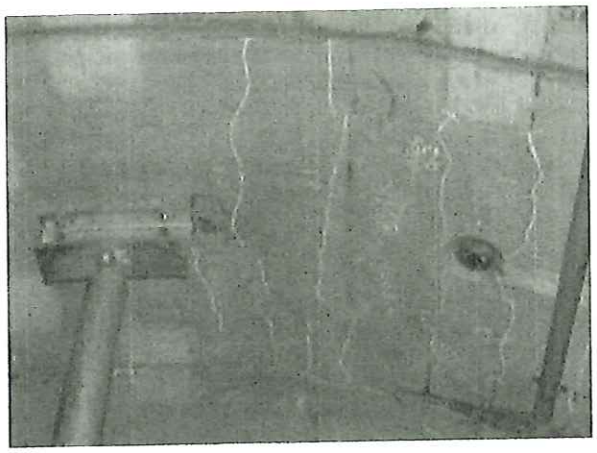

Figure 1. Longitudinal cracks on a segment.

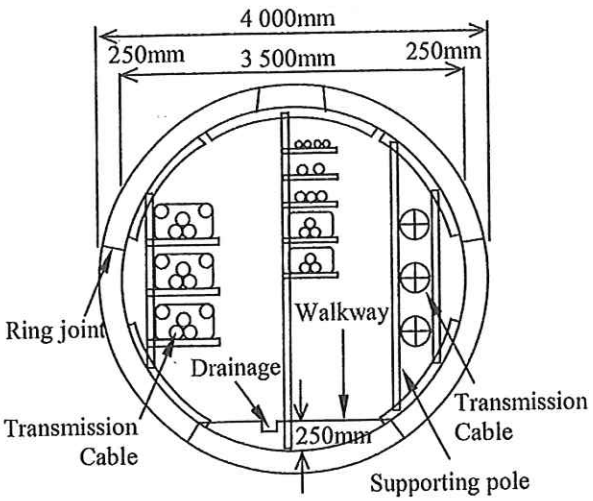

Figure 2. Cross-section outline of the target tunnel.

Table 1. Structural profile of the target tunnel.

Parameter	Properties
Inner diameter	3,500 mm
Segment width	900 mm
Segment thickness	250 mm
Number of segments	6 segments/1 ring
Reinforcement (Outer side)	Flat steel plate (75 mm × 2 mm, SS400) @ 2 plates + SD295 ϕ13 mm @ 4 bars
Reinforcement (Inner side)	Flat steel plate (75 mm × 2 mm, SS400) @ 2 plates + SD295 ϕ13 mm @ 4 bars
Distance from extreme compression fiber to extreme tension steel	215 mm
Distribution reinforcement	SR235 ϕ9 mm @ 165 mm
Compressive strength of concrete	45 N/mm^2

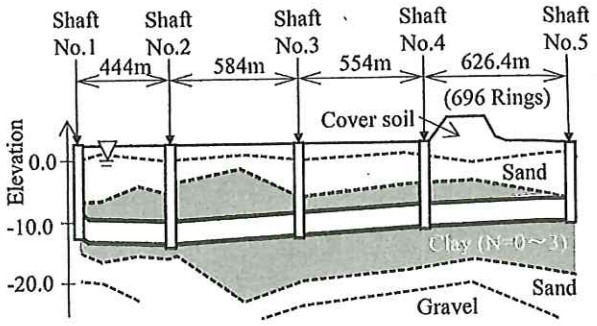

Figure 3. Longitudinal profile of the target tunnel.

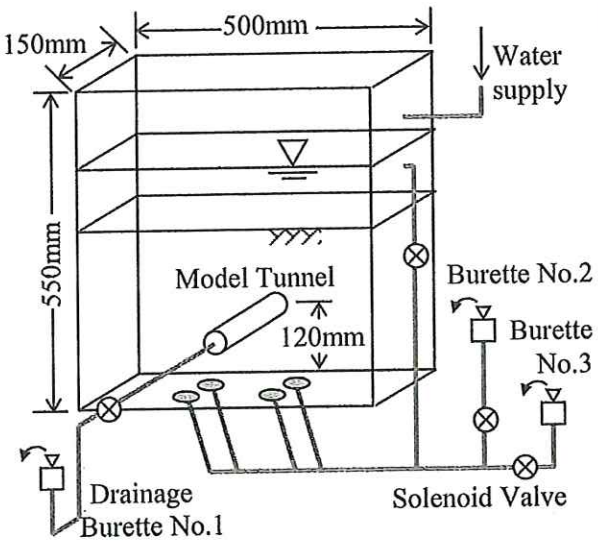

Figure 4. Experimental apparatus.

shown in Figure 5, they evaluated 1.3 as the "changed load ratio," where the changed load ratio was defined as shown (1).

$$\alpha = \frac{P_d + P_a}{P_d} \quad (1)$$

where α = changed load ratio; P_d = design load; and P_a = additional load.

Moreover, Kaneko et al. (2004) simulated this experiment with a two-dimensional analysis, and confirmed that the changed load ratio due to water leakage should be 1.3. Based on these results, they concluded that additional load should be generated by the relative displacement between the tunnel and side ground, causing a shear force the same as the concept by Marston and Anderson (1913), and Spangler (1948), as shown in Figure 6.

However, the water leakage shown in a field observation was not from the top, but mainly from the side and bottom. Additionally, the vertical inner displacement of this tunnel converges as shown in Figure 7.

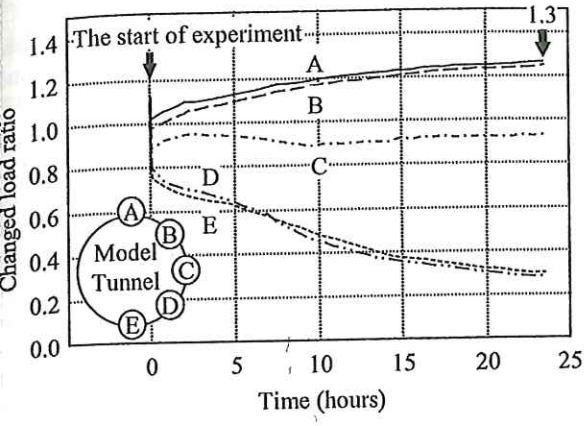

Figure 5. Variation of load change ratio with time.

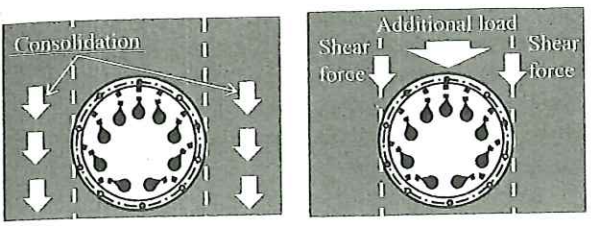

Figure 6. Mechanism of additional load in previous studies.

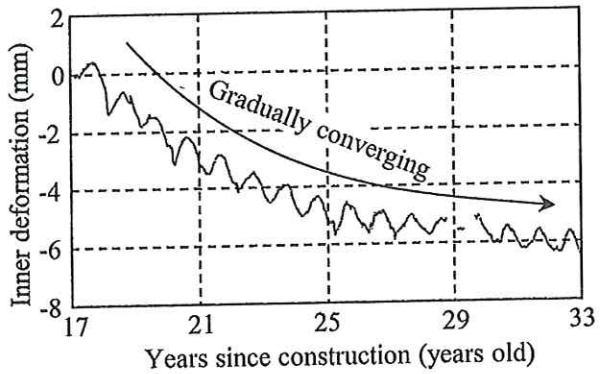

Figure 7. Inner displacement of target tunnel.

Therefore, it could be considered that the changed load ratio of 1.3 in previous studies was an overestimation.

4 CLARIFICATION OF ADDITIONAL LOAD USING THREE-DIMENSIONAL ANALYSIS

It was thought that the increase in water leakage should be deeply related to the increase in additional load on the top of the tunnel. Therefore, we first checked the tunnel's records of water leakage and deformation. We then assumed the mechanism of the additional load generated, based on the results of these checks. Finally, we confirmed, via three-dimensional analysis, the mechanism of the increase in additional load caused by ground consolidation due to the increase in water leakage.

4.1 *Records and mechanism assumptions*

4.1.1 *Tunnel records*

Figure 8 shows the range of stagnant water generated on the walkway of this tunnel due to water leakage at 10 years old and 34 years old. As shown in the figure, the range at 10 years old covered the section between rings No. 290 and No. 320. Additionally, the tunnel repair records at 10 years old said "water leakage started at 2 or 3 years old." Judging by this description, it is thought that the water leakage at 0 years old was very small, but then it gradually increased. In addition, the range of stagnant water eventually expanded to the section between rings No. 240 and No. 530, at 34 years old. Therefore, it is considered that the water leakage gradually increased day by day after the construction of this tunnel.

Secondly, Figure 9 shows the difference in elevation between the tunnel at 20 years old and 29 years old. This figure shows that the tunnel settled and that the maximum settlement was 11.9 mm. However, no large settlement was shown near shafts No. 4 or No. 5. The reason for this is considered to be that the tunnel is vertically fixed via these shafts.

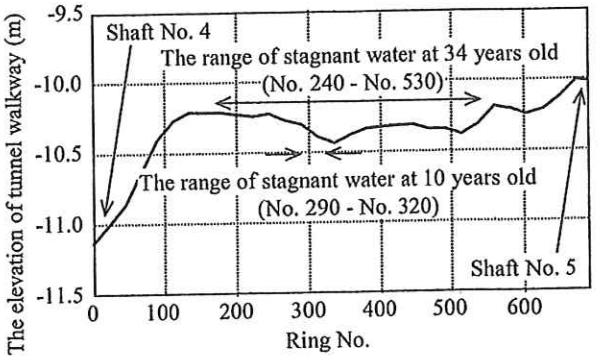

Figure 8. Range of stagnant water on walkway.

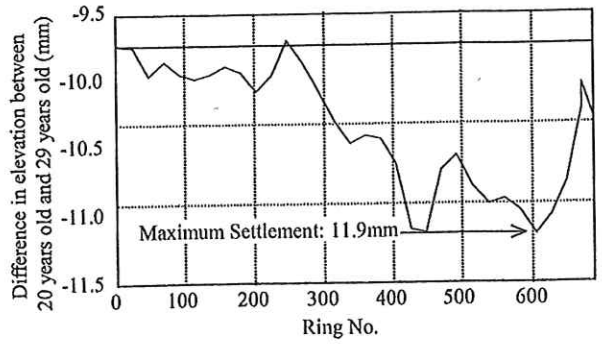

Figure 9. Record of the elevation difference.

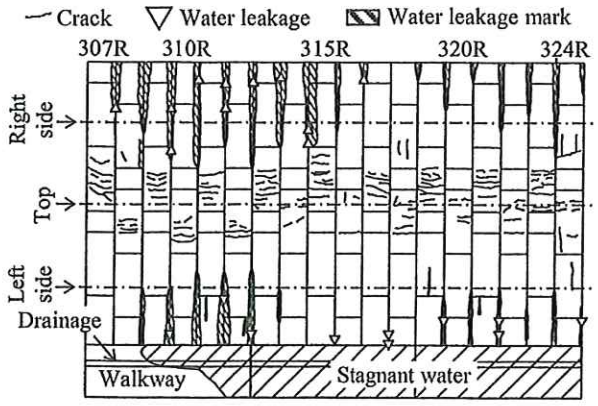

Figure 10. Sketching of cracks and water leakage.

Finally, Figure 10 shows the results of sketching out the cracks and water leakage from ring No. 307 to ring No. 324, at 24 years old. According to these records, most of the water leakage occurred from the ring joints in the lower half of the tunnel.

4.1.2 *Assumptions on the mechanism of the increase in additional load*

Based on these records, we assumed a mechanism in which the additional load increased with the consolidation of the ground due to water leakage, as shown in Figure 11.

First of all, a very small amount of water leakage into the tunnel happened at 0 years old, shown as STATE (A). As a result of this state, the ground to the side of the tunnel began to be consolidated and settled, as per STATE (B). Then, as shown in STATE (C), shear force was generated at the interface between the area around the tunnel and the ground above it, generating additional load, which pushed the tunnel downward. These STATE (A) to STATE (C) were the same as the previous research shown in Figure 3. Due to the additional load, however, the tunnel, supported by shafts, settled in the center, as shown in STATE (D). Finally, this settlement promoted the opening of the ring joints in the lower half, as shown in STATE (E). As a result, it is thought that an increase in additional load was promoted by a repeating of the cycle from STATE (A) to STATE (E).

This cycle of increase in additional load should converge when the consolidation of the ground due to water leakage has been completed. In order to verify this assumption, we employed a three-dimensional analysis that could clarify where and when additional load and water leakage occurred in this tunnel.

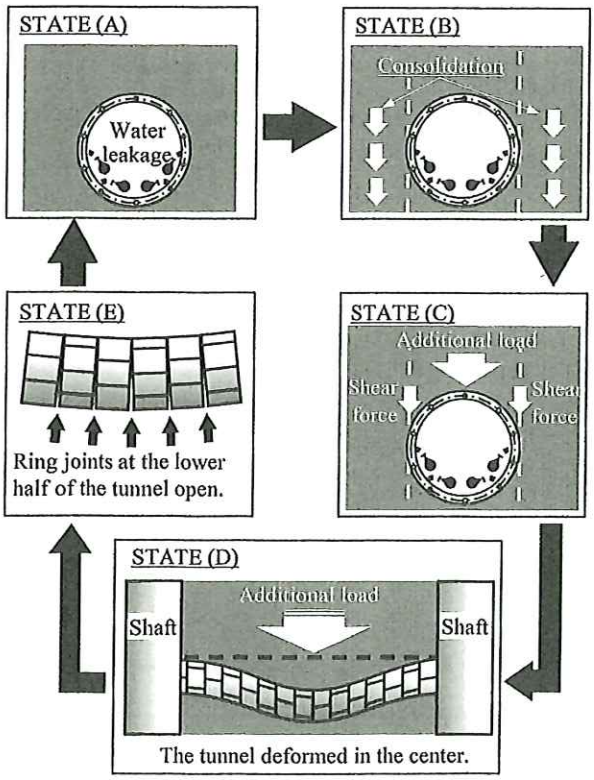

Figure 11. Assumptions on mechanism.

4.2 *Simulation model used in the three-dimensional analysis*

4.2.1 *Simulation model used*

Figure 12 shows the simulation model used in the three-dimensional analysis. In this simulation, each soil layer was composed of solid elements and the tunnel is expressed as a shell model between shafts No. 4 to No. 5. The analysis code used was a general ground analysis system, "Midas GTS NX." This model has 157,280 nodes, 16,704 shell elements for the tunnel, and 59,413 solid elements for the ground.

Tables 2 and 3 show the physical properties of the ground that were input. All physical property values were based on the results of a field survey. In order to properly evaluate the consolidation characteristics of the soil layer around the tunnel, a modified Cam-Clay model was applied. The other soil layers, however, were expressed as elastic bodies for the convergence in the calculation. Additionally, permeability in the horizontal direction was assumed to be twice

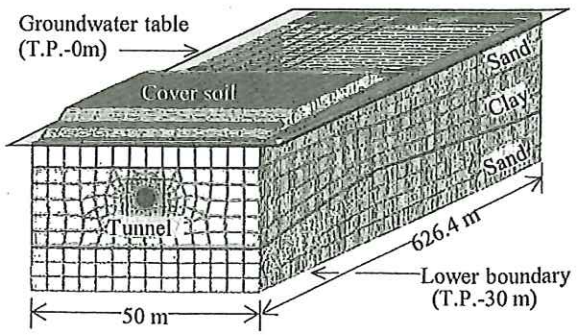

Figure 12. Simulation model used.

Table 2. Physical properties of the clay.

Parameter	Properties	
Unit Weight	16.4	kN/m^3
Ratio of the gradient of swelling line with respect to normal consolidation line	0.924	
Critical state coefficient	1.410	
Dilatancy coefficient	0.065	
Poisson's ratio	0.317	
Vertical permeability	4.11×10^{-9}	m/s
Horizontal permeability	8.22×10^{-9}	m/s
Static earth pressure coefficient	0.464	
Void ratio	1.353	

Table 3. Physical properties of other soil layers.

Parameter / Soil layer	Unit	Properties: Cover soil	Upper sand	Lower sand
Average layer thickness	m	1.9	5.5	4.6
Unit Weight	kN/m^3	17.5	17.5	17.5
Modulus of deformation	kN/m^2	9,300	4,000	4,000
Poisson's ratio	-	0.330	0.330	0.330
Permeability	m/s	4.11×10^{-9}	4.24×10^{-5}	5.90×10^{-6}
Void ratio	-	1.105	1.105	1.105

that of the vertical direction in the soil layer in which the tunnel existed, according to Tsutsui et al. In other soil layers, it was assumed that permeability in the horizontal direction was the same as in the vertical direction.

Table 4 shows the physical properties of the tunnel that were input. The equivalent rigidity of the shell model, which was assumed to reduce due to the ring joints, was calculated based on the guidelines for earthquake resistance measures for sewerage facilities.

The boundary condition was that the vertical direction of the tunnel was fixed at its ends, i.e. shafts No. 4 and No. 5. The sides of the whole model were fixed in the horizontal direction, and the bottom was fixed in all directions. The groundwater level in this simulation was assumed constant for every year.

Table 4. Physical properties of the tunnel.

Parameter	Properties
Unit Weight	24 kN/m^3
Equivalent rigidity	5.88×10^7 kN•m^2
Poisson's ratio	0.30

4.2.2 *Modeling of water leakage*

The following 3 points were assumed for water leakage into the tunnel.

The first point is the assumption of the initial water leakage location noted in STATE (A) of Figure 11. As shown in Figure 13, these initial locations were assumed to be the same as 8 large water leakages observed in a field survey at 24 years old. The water leakage near shaft No. 5 was discounted, because this leakage should not have been from the ring joints, but from shaft No. 5.

The second point is how to judge if water leakage had started or not. Figure 14 shows the results of pore water pressure measurements from 26 years old to 30 years old at ring No. 317. According to this, pore water pressure was 115 kPa when the joint opening was 0.114 mm, and 105 kPa with the joint opening closed. Both pore water pressures were less than the theoretical pore water pressure of 130 kPa. Therefore, as shown in Figure 15, it was assumed that the point when the joint opening became 0.228 mm could be judged to be the start of water leakage.

The final point is the pore water pressure when the joint opening becomes 0.228 mm. In this study, it was assumed that the water leakage location should be a free drainage condition and that pore water pressure should drop to 0 kPa.

Additionally, as shown in Figure 16, the water leakage from the upper half of the tunnel was

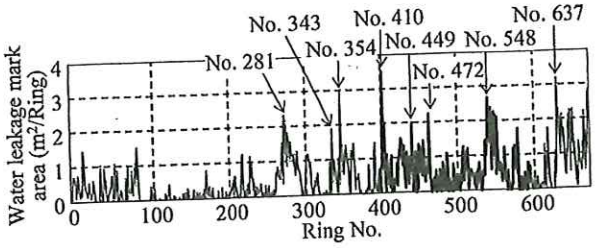

Figure 13. Distribution of water leakage marks.

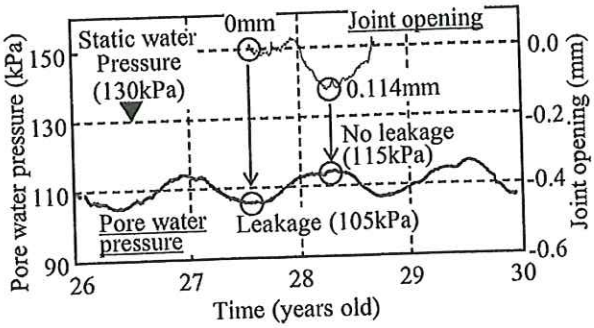

Figure 14. Measurement results at ring No. 317.

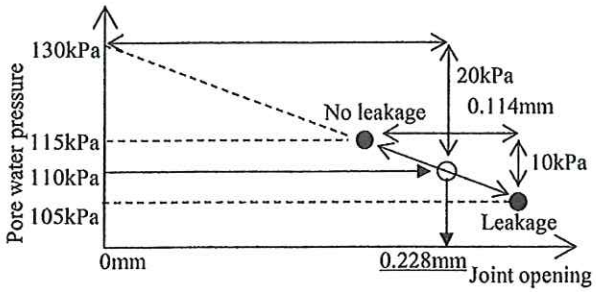

Figure 15. Joint opening at the start of water leakage.

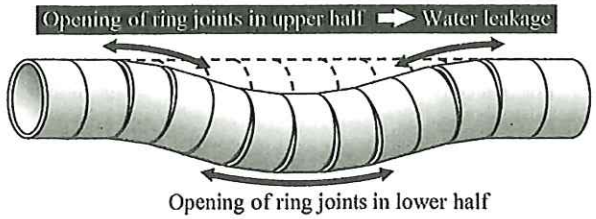

Figure 16. Water leakage in upper half.

assumed to be the same as in the lower half. The timings of joint openings are judged to be at 0, 7, 15, 20, 29, 36, 39 and 49 years old.

4.2.3 *Analysis results*

First, Figure 17 shows the analysis results of the settlement from 20 years old to 29 years old with a field survey. As shown in the figure, the analysis results simulated the field survey well, but a slight difference can be recognized. For example, near ring No. 440, the analysis result was 18.2 mm with respect to the actual measurement of 11.8 mm. Also, near shaft No. 5, the analysis result was 20.3 mm, larger than the actual settlement of 11.9 mm. The reason for this difference is thought to be that assumptions regarding the pore water pressure of 0 kPa at joint opening could be different from the actual conditions. Aside from these differences, however, the analysis model was able to simulate the overall tendencies of the actual phenomenon in this tunnel.

Secondly, Figure 18 shows the calculated change in the tunnel's longitudinal profile for 15 years old, 20

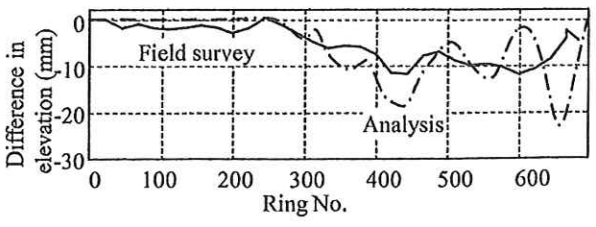

Figure 17. Results of comparison analysis with field survey.

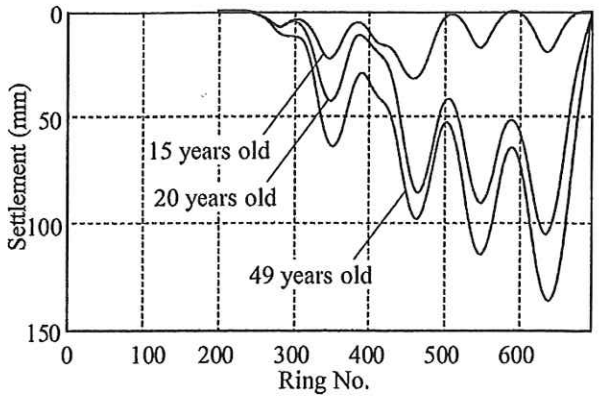

Figure 18. Calculated settlement for each year.

years old and 49 years old. As shown in this figure, it was found that the settlement converged after 20 years.

Thirdly, we confirmed the change in hydraulic gradient due to water leakage. Figures 19 and 20 show the changes in hydraulic gradient near ring No. 329, where no water leakage occurred, and ring No. 343, which is assumed to be the initial water leakage location. For ring No. 329, the hydraulic gradient mostly did not change. Near ring No. 343, however, a steep gradient, which mostly converged at 15 years old, was calculated. It can be thought that a steady and constant groundwater flow toward the tunnel had been generated. Therefore, it is considered that once the consolidation of ground has been completed the additional load should converge as the hydraulic gradient becomes constant, i.e. the water leakage becomes a steady flow.

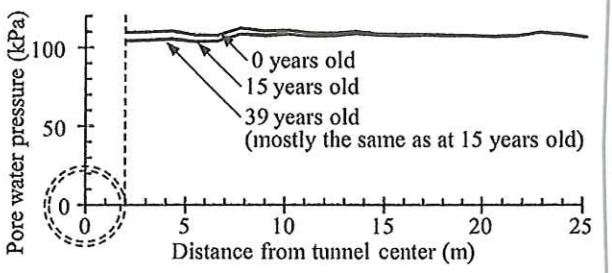

Figure 19. Calculated hydraulic gradient at ring No. 329.

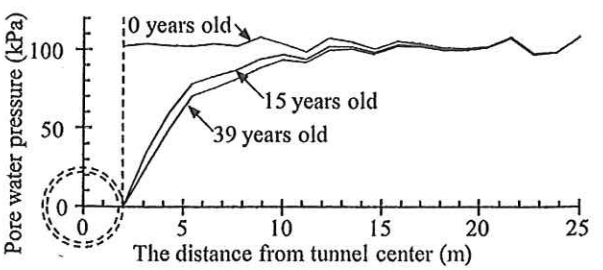

Figure 20. Calculated hydraulic gradient at ring No. 343.

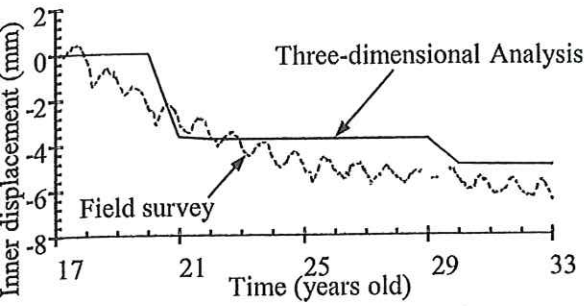

Figure 21. Inner displacement of ring No. 311.

Finally, Figure 21 shows the three-dimensional analysis results for the inner displacement of ring No. 311 with the field survey. As shown in the figure, the three-dimensional analysis simulated the field results well, and it seems that the inner displacement is converging with time. Therefore, it seems that convergence of the additional load can be assumed.

5 PROPOSAL OF SIMPLE METHOD VIA TWO-DIMENSIONAL ANALYSIS

In this chapter, a simple calculation method for the changed load ratio using a two-dimensional analysis is proposed, based on the analysis results using the three-dimensional model.

5.1 *Outline of proposed method*

Figure 22 shows the procedure for the simple method proposed in this study.

First, as shown in PROCEDURE (A), the annual average pore water pressure near the tunnel is measured. In the case of this tunnel, the total water head difference from the groundwater table was 3.5 m at 26 years old, since the pore water pressure measured 35 kPa lower than the hydrostatic pressure. In PROCEDURE (B), the first-order approximating solution of the consolidation formula is fitted to the measurement results of the change in the internal displacement of a tunnel. After PROCEDURE (B), to predict how much the total water head difference will become in the future, this fitted graph curve is applied to the change in total water head difference, as shown in PROCEDURE (C). In this case, it was predicted to converge at 4.0 m. The total water head difference should be 0m at 0 years old, 3.5 m at 26 years old, and 4.0 m in the future. Finally, as shown in PROCEDURE (D), approximating with polygonal lines, a change in the total water head difference of 4.0 m at 30 years old is calculated. By inputting these polygonal lines into the two-dimensional analysis, as shown in Figure 23, the change in the changed load ratio can be calculated.

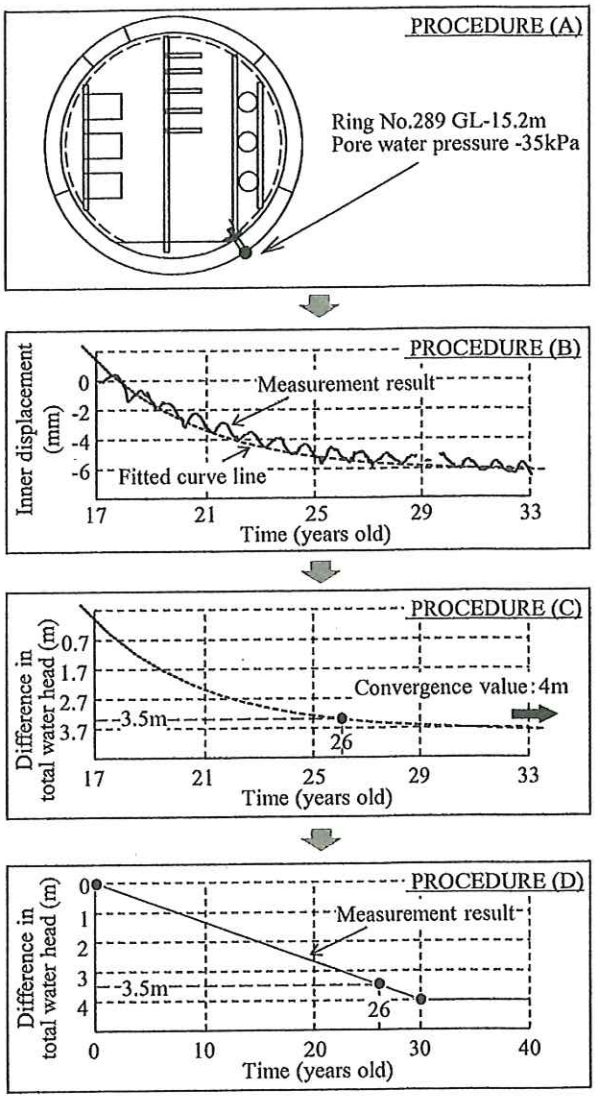

Figure 22. Flow chart of our proposal method.

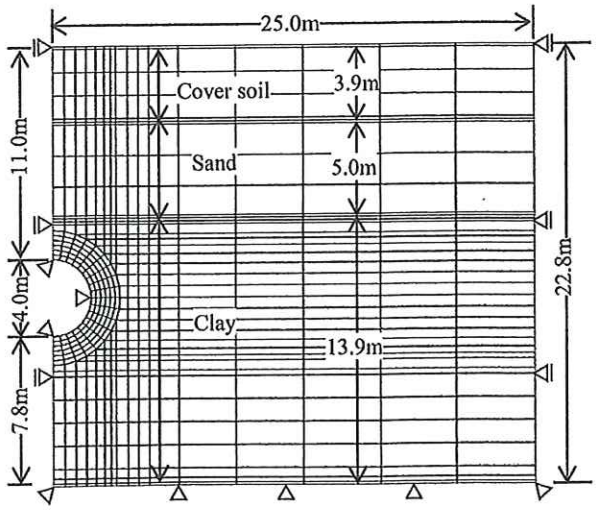

Figure 23. The model for two-dimensional analysis.

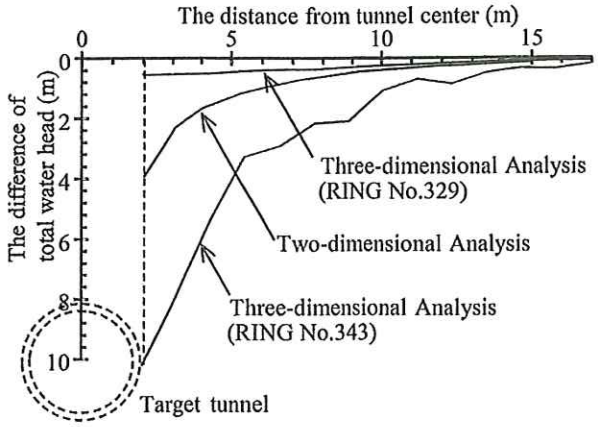

Figure 24. Calculated results for each analysis.

5.2 *Comparing the results of the simple method with the three-dimensional analysis*

Figure 24 shows the results of comparing the analysis results for the hydraulic gradient using the simple method and three-dimensional analysis. The results of three-dimensional analysis concern ring No. 329 and ring No. 343. As shown in the figure, the result of two-dimensional analysis result is nearly same as that of three-dimensional analysis.

Also, Figure 25 shows the analysis results for the changed load ratio calculated using two-dimensional analysis and three-dimensional analysis at ring No. 329, in which the value of settlement is mostly equal to the average value of all rings. These changed load ratios converged between 1.08 and 1.09 in both analyses. It can be evaluated that the results of the simple method are mostly the same as those of the three-dimensional analysis.

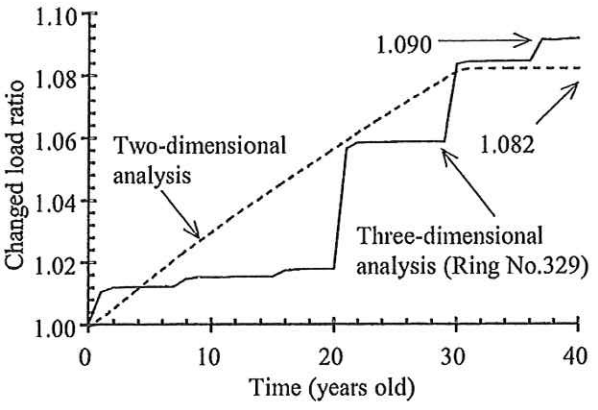

Figure 25. Calculated changed load ratio.

6 CONCLUSION

In the consolidation of the surrounding ground due to water leakage into the tunnel, an increase in additional load is promoted via a mechanism where ring joint opening occurs in the lower half of the tunnel when the tunnel settles. Additionally, the additional load generated by the water leakage into the tunnel eventually becomes constant with the convergence of the hydraulic gradient. Moreover, using the two-dimensional analysis method proposed in this study, the convergence value of the changed load ratio can be predicted.

We plan to apply the results of this study in order to design suitable countermeasures to reinforce tunnels in certain years.

REFERENCES

Ariizumi, T., Kaneko, S., & Enya, Y. 2006. The study on long term load of a shield tunnel. *Tunnels and Underground, 37* (11), 49–56.

Enya, Y., Naito, Y., Anan, K., Ootsuka, M., & Koizumi, A. 2011. Study of reinforcement design for deteriorated shield tunnel. *Journal of JSCE, 67*(2), 62–78.

Japan Sewage Works Association. 2014. The Guidelines For Earthquake Resistance Measures For Sewerage Facilities, 172–174.

Kaneko, S., Ariizumi, T., Yamazaki, T. & Enya, Y. 2004. Earth pressure on shield tunnel lining induced by settlement due to consolidation of soft clay. *Proceedings of the Symposium on Underground Space, Vol.9*, 227–234.

Marston, A. & Anderson, A.O. 1913. The theory of loads on pipe in ditches and tests of cement and clay drain tile and sewer pipe, *Bulletin*, 31, Iowa Eng. Experiment Station.

MIDAS IT Japan Co., Ltd. 2018. 64-bit geotechnical analysis system "Midas GTS NX."

Spangler, M. G. 1948. Underground conduits - An appraisal of modern research, *Transactions of ASCE, 113* (2337). 316–374.

Takiyama, K., Komiya, K., & Akagi, H. 2006. Finite element analysis on the settlement behavior of a shield tunnel in soft clay ground. *Journal of JSCE, 16*, 111–120.

Tsutsui, Y., Tanaka, H., & Yamazoe, N. 2014. The anisotropy of permeability checked by a triaxial tester, *Technical Report of Geotechnical Engineering Association Hokkaido*, 54. 41–44.

Yakita, S., Nakayama, T., Nakayama, T., Tsuno, K., Takahashi, H., Komiya, K., & Akagi, H. 2013. Long term deformation analysis of a shield tunnel due to consolidation settlement considering crack induced stiffness reduction. *Journal of JSCE, 69*(4), 457–468.